

25<sup>th</sup> ABCM International Congress of Mechanical Engineering  
October 20-25, 2019, Uberlândia, MG, Brazil

## COB-2019-1706 NUMERICAL ANALYSIS OF A POINT ABSORBER UNDER REGULAR WAVES

**Paulo Fiuza Lamarão**

**Alexandre Stefano Menegazzo**

**Leonardo Cardim Pazim**

**Walter Jesus Paucar Casas**

Universidade Federal do Rio Grande do Sul – UFRGS, R. Sarmento Leite, 425 - Centro Histórico, Porto Alegre - RS, 90050-170  
paulo.lamarao@ufrgs.br, alexandre.menegazzo@gmail.com, pazimleonardo@gmail.com, walter.paucar.casas@ufrgs.br

**Victorio Nardin**

Universidade Federal do Rio Grande, Av. Itália, s/n - Km 8 - Carreiros, Rio Grande – RS, CEP 96203-900  
vnardin94@gmail.com

**Abstract.** *Due the great potential of energy generated by waves, the search for principles of conversion for this type of energy is the subject of much research. It is known that oscillating body systems are able to take advantage of the energetic potential of waves in the open sea. Therefore, they represent an alternative for devices installed near or on-shore, such as water column devices and reservoirs filled by wave actions. Thus, the objective of this paper consists in a numerical analysis of the behavior and the energetic potential of a Point Absorber (PA) device fully submerged under the Airy wave's action. The development of this paper includes numerical simulation made with the Ansys AQWA software to obtain the hydrodynamic properties of the system. The validation of the mesh refinement and of the time step was made. The wave parameters and the dimensions of the system were chosen in order to enable a posterior comparison with the experimental analysis in a wave tank. The graphs of position, frequency spectrum, force at the spring and potential energy were plotted for different wave parameters. From an oscillatory point of view, the system presented itself as stable, with a great potential for energy generation. However, the difference in the values of power for the simulated cases show the great challenge in obtaining a configuration optimized for the wave regime of a specific region.*

**Keywords:** *point absorber, wave energy, numerical simulation*

### 1. INTRODUCTION

Due to the great necessity of replacement for the use of fossil fuels, the enhancement of renewable energy converters is a recurrent subject of research in engineering. However, regarding wave energy conversion, a consensus is yet to be achieved. It is known that the total theoretical wave energy potential is estimated to be 32,000 TWh/yr (Mørk et al., 2010), with the global technical potential of wave energy being of about 500 GW (Sims et al., 2007), assuming offshore wave energy devices with an efficiency of 40% and that they are only installed near coastlines with wave climates of more than 30 kW/m. Therefore, there is a great potential of wave energy generation to be explored.

Numerous types of devices have been researched and, according to Falcão (2009), can be classified by their principles of operation: Oscillating Water Column; Oscillating Body and Overtopping. This paper focuses on the numerical analysis of a Point Absorber, a specific kind of Oscillating Body System.

These devices can be partially or fully submerged, the latter being less used due its small energy generation capacity and the complex movements caused by the different degrees of freedom of the system. As shown by Budal and Falnes (1982) and Naito and Nakamura (1986), the optimal configuration that maximizes the wave power absorbed requires a precise control of the oscillation, which can be done in a hydrodynamic simulation.

### 2. MODELLING

Initially, based on the size of the wave tank used in the experimental analysis and its range of operations, the wave parameters and dimensions of the PA and cable were set. The values utilized satisfy also the linear theory of Airy waves and were calculated accordingly to the Ursell parameter, with the deep sea conditions determined from Dean and Dalrymple (1991).

Figure 1 show the system composed by the tank and PA. The modelling was made with the Ansys AQWA software and the dimensions of the tank and PA are  $b = 16$  m;  $w = 0.71$  m;  $h = 0.6$  m,  $d = 0.08$  m and mass  $m = 1$  kg. The diameter used was chosen in order to maintain the blockage ratio smaller than 12% to avoid large scattering with the walls of the tank, according to Sergiienko and Ding (2017). Three different depths for the installation of the PA were determined according to the medium wave height level. In order to assure the fully submerged condition of the PA, the maximum and minimum depths were set as 0.25 m and 0.15 m, respectively, with an intermediate value of 0.20 m. Regarding the wave parameters used, the wave amplitude chosen was of  $A = 0.055$  m and the wave periods were of  $T = 0.75$ ; 0,80 and 0.85 s.

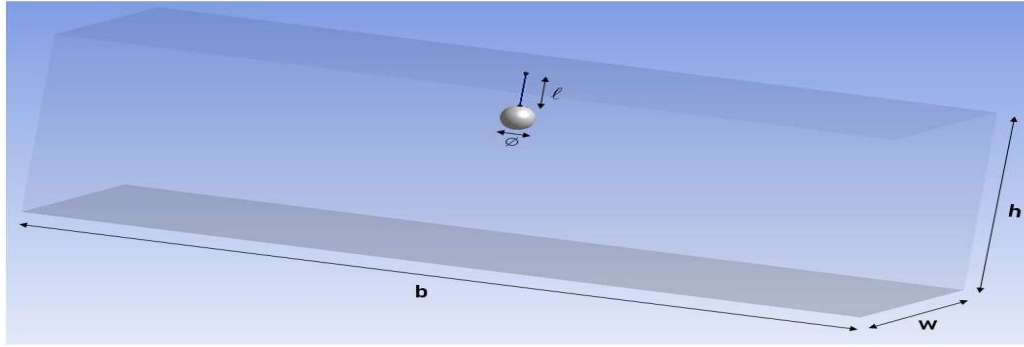


Figure 1. Modelling of the wave tank and Point Absorber.

The numerical modelling of the submerged structure's behavior was based on a mass-spring-damper system with forced vibration caused by hydrodynamic forces of waves in the horizontal and vertical directions, with spring stiffness varying between 100,000 N/m (undeformable cable), 200 N/m, and 400 N/m, in addition with the initial load applied in the spring element due the difference between the weight and the buoyancy of the body, as can be seen in the equation below:

$$M_T \ddot{x}(t) + C \dot{x}(t) + Kx(t) = F_{ext}(t) \quad (1)$$

where  $M_T$  is the sum of the structural and additional mass;  $C$  is the viscous damping;  $K$  is the cable stiffness, modelled as a spring. The excitation force is described as:

$$F_{ext}(t) = F_{fk}(t) + F_m(t) + F_{e-p} \quad (2)$$

where  $F_{fk}$  is the Froude Krylov force;  $F_m$  is the Morison force and  $F_{e-p}$  is the difference between weight and buoyancy.

According to Chakrabarti (1987), the Morison force for structures free to move is determined by Eq. (3), known as the Morison Equation:

$$F_m = C_m A_t \dot{u} - C_A A_t \ddot{x} + C_D A_D |u - \dot{x}|(u - \dot{x}) \quad (3)$$

with  $C_m$ ,  $C_A$  and  $C_D$  being the inertia, additional mass and drag coefficients, respectively, and  $u$  the velocity of the water particle in the horizontal direction. Also,  $A_t$  and  $A_d$  are given by:

$$A_t = \frac{\rho \pi D^2}{4} \quad (4)$$

$$A_D = \frac{\rho D}{2} \quad (5)$$

with  $D$  being the sphere's diameter. As previously mentioned, the model considers only the excitations caused by Airy waves in deep water regimes. Therefore, the kinematics of the water particle in the  $x$  and  $z$  directions and the dynamic pressure are described by Eq. (6), (7) and (8), respectively.

$$u = \frac{H\sigma \cosh k(h+z)}{2\sigma \sinh(kh)} \cos(kx - \sigma t) \quad (6)$$

$$w = \frac{H\sigma \operatorname{se}^{-\sigma(h+z)}}{2\operatorname{senh}(kh)} \operatorname{sen}(kx - \sigma t) \quad (7)$$

$$P_d = \rho g \frac{H\sigma \cos(kx - \sigma t)}{2\operatorname{sen}(kh)} \cos(kx - \sigma t) \quad (8)$$

with  $H$  being the wave height,  $k$  the wave number,  $\sigma$  the wave angular frequency,  $\rho$  the water density and  $g$  the acceleration of gravity. The external forces corresponding to the Froude-Krilov part are determined by an integration of the dynamic pressure, Eq. (8), resulting in the following equations:

$$F_{fkx} = C_H \iint_S P_d n_x ds = C_H \rho \dot{w} V_{esf} \quad (9)$$

$$F_{fkz} = C_V \iint_S P_d n_z ds = C_V \rho \dot{w} V_{esf} \quad (10)$$

To determine the hydrodynamic coefficients used in the equations above, the AQWA software discretizes the body by dividing it in panels and, later, makes use of the Boundary Element Method to solve the differential equations.

### 3. MESH REFINEMENT VALIDATION AND DETERMINATION OF THE TIME STEP

In order to determine some hydrodynamic parameters, as, for instance, the added mass matrix of the PA, the AQWA software makes a discretization of the body. Therefore, a mesh validation is required, and this was done based on the determination of the structural mass needed by the body to be at total hydrostatic equilibrium at the desired depth. Beginning with a coarse mesh, the number of elements and structural mass data were plotted in order to analyze the convergence of the mass value, as seen in Fig. 2.

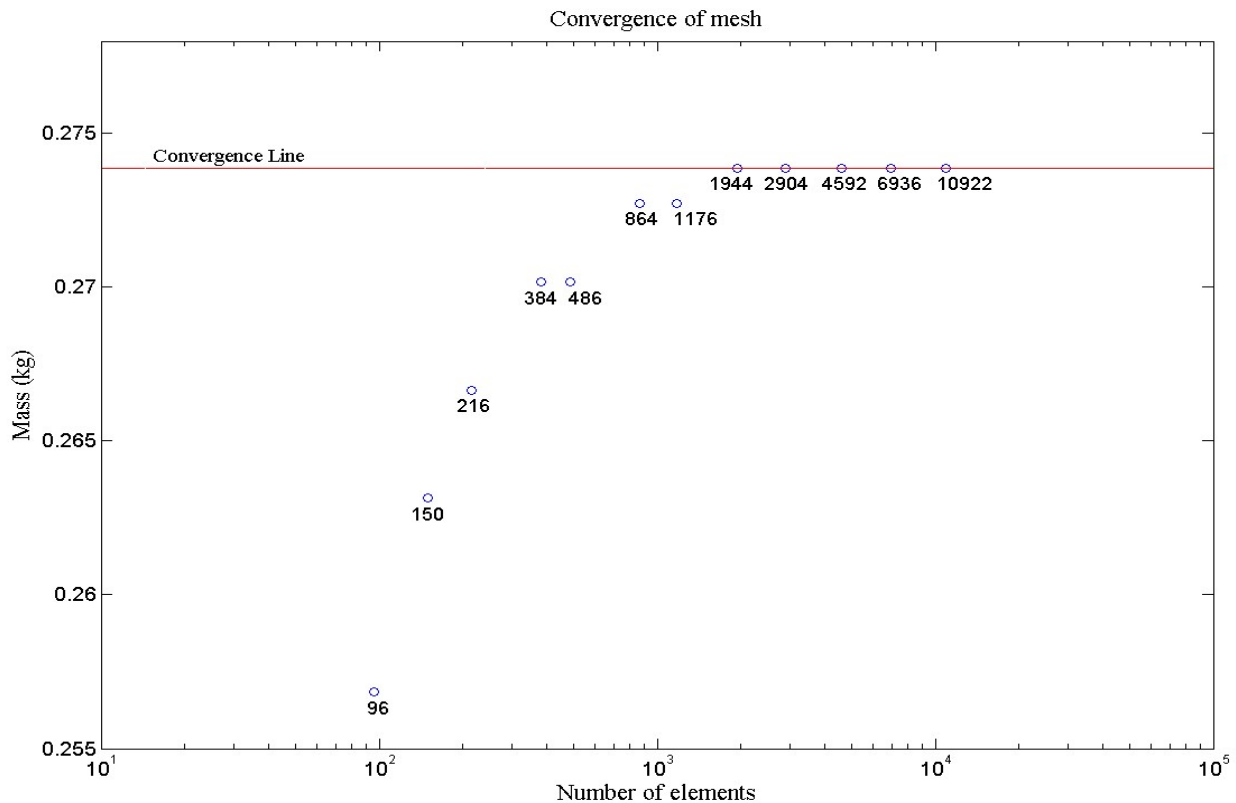


Figure 2. Mass of the structure for each mesh.

With the convergence of the mass value, it was verified that the ideal mesh refinement for the PA's surface was the one with 2904 squared elements. With the proper mesh set, the time step for the temporal analysis was determined.

Wave conditions of period of 0.85 s, amplitude of 0.075 m and body depth of 0.2 m were used, with the values of time step varying from 0.01 s to 0.0008 s with total duration of 60 seconds. The values of position along the Z axis as function of time were plotted using MATLAB in order to perform the stability analysis (Fig. 3).

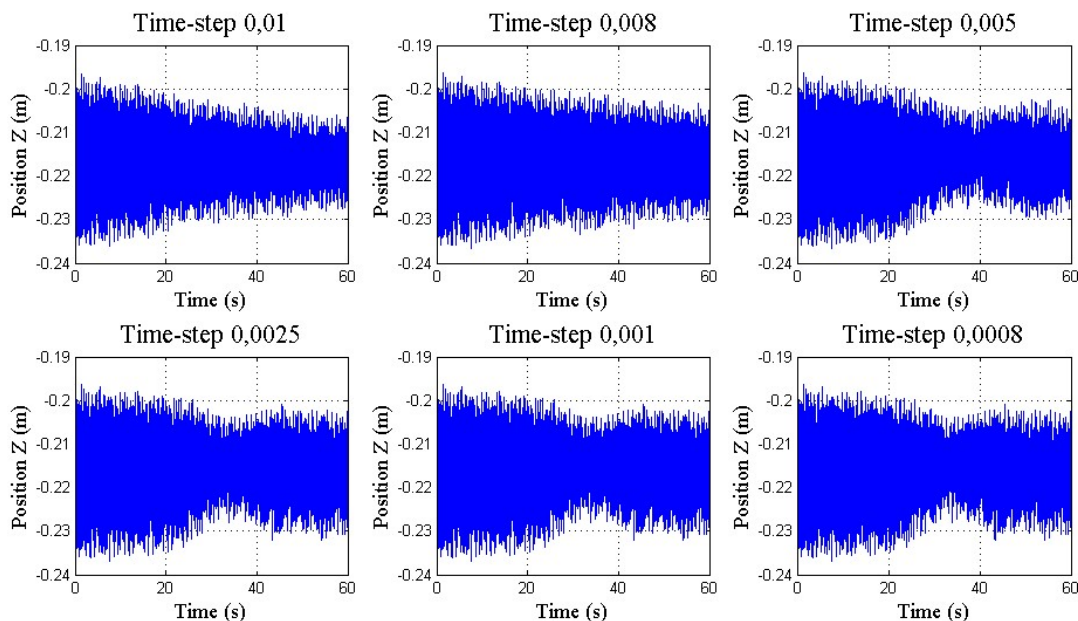


Figure 3. Position of the body for different time steps.

The graphs show that, from the time step equal to 0.0025 s, there was no significant variation in the response of the position with a change in the time step. Therefore, the time step for the simulations was fixed as 0.0025 s.

#### 4. SIMULATION

In this stage, 27 cases were simulated, with a variation of spring stiffness of 100000, 200, and 400 N/m, periods of 0.75, 0.80, and 0.85 s and body depth of 0.15, 0.20, and 0.25 m, in order to evaluate the influence of these parameters in the behavior of the structure and the amount of energy generated.

#### 5. RESULTS AND DISCUSSION

Graphs for position versus time of two predominant degrees of freedom as well the strength in the cable and their spectrum of frequency were plotted, as shown for one of the cases in the graph below (Fig. 4). It was observed that in all cases the structure response presents a transient and a permanent behavior. The transient part represents the portion of free vibration, caused by the load of the difference of the weight of the PA and the buoyancy, while the permanent portion is caused by the hydrodynamic wave forces.

The simulation and the initial analysis of the structure's response presented values of instantaneous force on the cable, as shown in Fig. 4. It was considered that only the permanent part of the simulation would be utilized to determine the elastic potential energy, in order to disconsider the effects of free vibration. Then, these data were derived using the Finite Difference Method for obtaining the instantaneous power. In order to quantify the energy that can be utilized by different electrical energy converters, only the positive averages of power were considered. Table 1 presents the power values according to the variation of each of the parameters described.

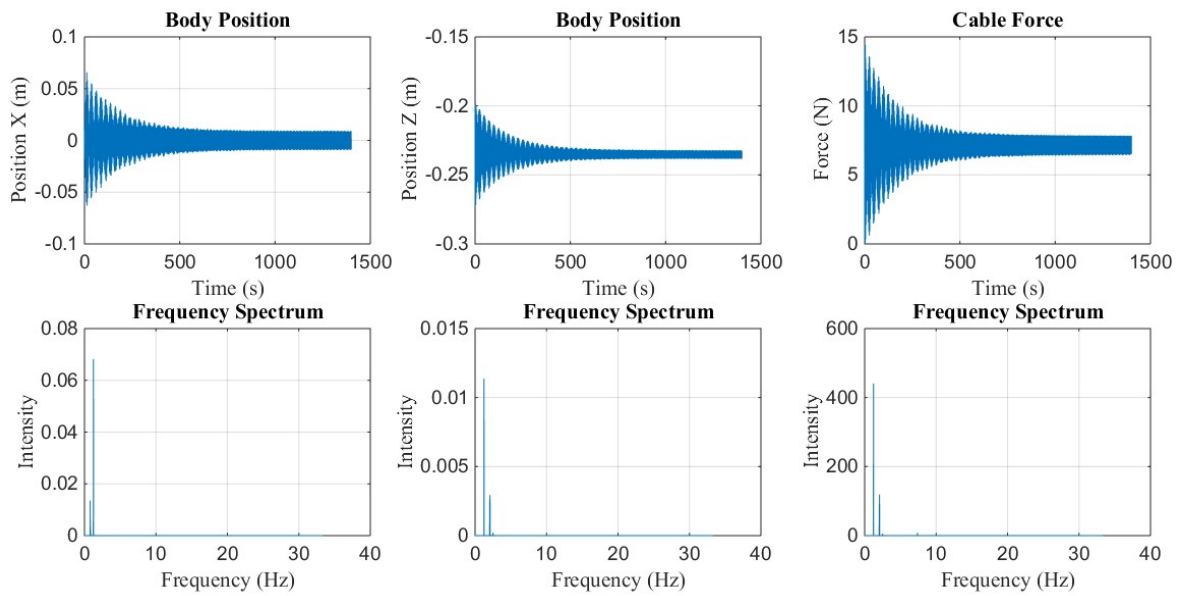


Figure 4. Body Position, Cable Force and Frequency Spectrum for deepness of 0.20 m, stiffness of 200 N/m and period of 0.80 s.

Table 1. Power values according to the variation of cable stiffness, water depth and wave period.

Cable stiffness (N/m)	Water depth (m)	Period (s)	Power (W/h)
100,000.00	0.25	0.85	1.45
		0.80	1.45
		0.75	1.45
	0.20	0.85	1.48
		0.80	1.50
		0.75	1.48
	0.15	0.85	1.89
		0.80	1.66
		0.75	2.19
200.00	0.25	0.85	8.22
		0.80	9.25
		0.75	11.71
	0.20	0.85	23.27
		0.80	33.86
		0.75	16.46
	0.15	0.85	188.87
		0.80	91.96

		0.75	62.69
400.00	0.25	0.85	2.86
		0.80	3.48
		0.75	5.34
	0.20	0.85	5.00
		0.80	5.00
		0.75	9.36
	0.15	0.85	891.80
		0.80	691.38
		0.75	557.22

Comparing the results shown at Tab. 1, it is observed that a nonlinear increase of the power occurs when the water depth decreases. Furthermore, in most of the cases, there is an increase of the power proportional to the increase of the wave period.

This is an expected result, since the velocity of the water particle (Eqs. (6) and (7)), that is already nonlinear, is squared in the Morison equation (Eq. (3)). This behavior is shown in Fig. 5.

Regarding the different stiffness parameters, it is noticed that the condition of undeformed cable has the minimum values of power in relation to the cable stiffness of 200 and 400 N/m (red values).

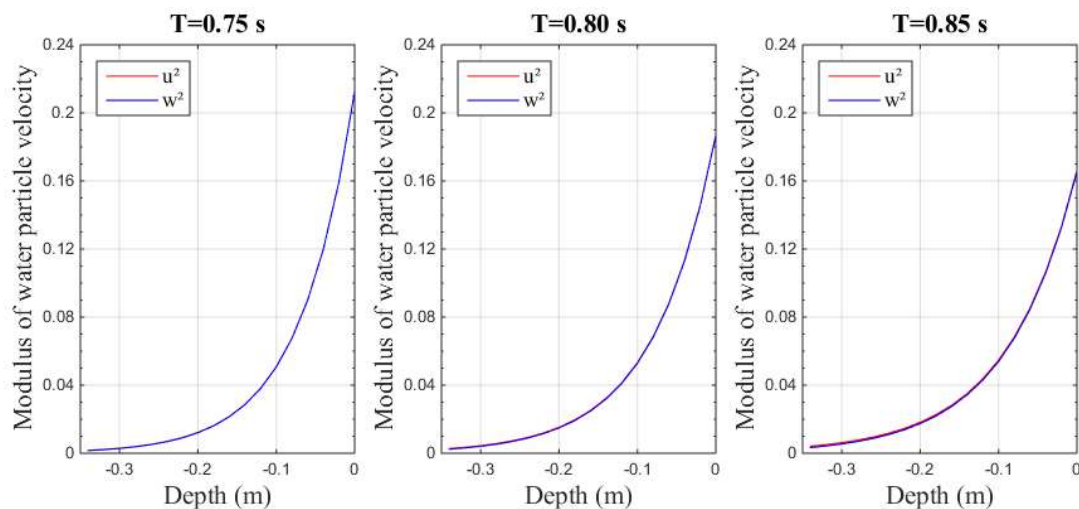


Figure 5. Variation of the velocity squared with the water depth and wave period.

## 6. CONCLUSIONS

The results of the alternating system of the oscillating body showed that for none of the parameters simulated situations near resonance or instability were encountered. This result satisfies the first objective of this work. It can be concluded as well that the greatest potential of energy generation was found for the cases with cables of 400 N/m of stiffness. This could be originated by the fact that the natural frequency of the system is closer to the excitation frequency.

It is interesting to note the great potential for energy generation presented by this mechanism, as can be seen in the result of power for the case of 400 N/m of stiffness, 0.15 m of depth and wave period of 0.85 s. However, due the large difference in power for different cases, the greatest challenge in the use of this type of converter is precisely in determining the set of parameters that present the biggest potential of energy generation for a specific wave regime.

The AQWA simulations presented themselves in accordance with the expected behavior, according to the model equations and the experimental validation. It can be seen that the system with the suspended oscillating body appears to present more benefits than a system with buoys, as the latter requires a proper fixation in the seabed.

## 7. ACKNOWLEDGEMENTS

This study was financed in part by the Coordination for the Improvement of Higher Education Personnel – Brasil (CAPES) – Finance Code 001, the National Council for Scientific and Technological Development (CNPq) and Rio Grande do Sul State Research Support Foundation (FAPERGS).

## 8. REFERENCES

- Chakrabarti, S. K., 1987. *Hydrodynamics of offshore structures*. WIT press, London, UK 1 First edition.
- Dean, R. G., & Dalrymple, R. A. 1991. *Water wave mechanics for engineers and scientists*. World Scientific Publishing Company, London, Vol. 2.
- Falcão, A. F. O., 2009. “The development of wave energy utilisation”. *IEA-OES Anual Report*, pp. 30-37.
- Falnes, J. and Budal K., 1982. “Wave-power absorption by parallel rows of interacting oscillating bodies”. *Applied Ocean Research*, Vol. 4, No. 4, pp. 194-207.
- Mork, G., Barstow, S., Kabuth, A., & Pontes, M. T., 2010. “Assessing the global wave energy potential”. In *ASME 2010 29th International conference on ocean, offshore and arctic engineering - ASME 2010*. Shanghai, China.
- Naito, S., & Nakamura, S., 1986. “Wave energy absorption in irregular waves by feed forward control system”. In *Hydrodynamics of ocean wave-energy utilization*, pp. 269-280. Springer, Berlin, Heidelberg.
- Sergiienko, N. Y., Cazzolato, B. S., Ding, B., Hardy, P., & Arjomandi, M., 2017. “Performance comparison of the floating and fully submerged quasi-point absorber wave energy converters”. *Renewable Energy*, Vol. 108, pp. 425-437.
- Sims, R. E., Schock, R. N., Adegbulugbe, A., Fenhann, J. V., Konstantinaviciute, I., Moomaw, W., ... & Uchiyama, Y. 2007. “Energy supply”. In *Climate change 2007: mitigation. Contribution of working group III to the fourth assessment report of the intergovernmental panel on climate change*. Cambridge University Press.

## 9. RESPONSIBILITY NOTICE

The authors are the only responsible for the printed material included in this paper.